General and Convenient Method for Making Highly Luminescent Sol−Gel Derived Silica and Alumina Films by Using LaF_3 Nanoparticles Doped with Lanthanide Ions (Er^{3+}, Nd^{3+}, and Ho^{3+})

V. Sudarsan, Sri Sivakumar, and Frank C. J. M. van Veggel*

Department of Chemistry, University of Victoria, P.O. Box 3065, Victoria, British Columbia, Canada, V8W 3V6

Mati Raudsepp

Department of Earth and Ocean Sciences, The University of British Columbia, Vancouver, British Columbia, Canada, V6T 1Z4

Received May 18, 2005. Revised Manuscript Received July 8, 2005

Silica films with Ln^{3+}-doped LaF_3 nanoparticles were prepared by sol gel method and their luminescent properties were studied as a function of the temperature. Significant improvements in the luminescent properties, in terms of the lifetime for the $^4I_{13/2}$ level of Er^{3+} (∼10.9 ms), $^4F_{3/2}$ level of Nd^{3+} (∼171 μs), and $^5F_3$ level of Ho^{3+} (∼6 μs), were obtained when corresponding nanoparticles are incorporated in silica films rather than the bare ions. In addition to the LaF_3 as the low phonon energy matrix, the absence of lanthanide ion clustering, and the increased distance between the OH groups of the silica matrix and the lanthanide ions, are responsible for the observed improvements in the luminescent properties for nanoparticle incorporated silica films. Lifetime values could be further improved by incorporating core−shell nanoparticles (the doped LaF_3 core surrounded by an undoped shell of LaF_3) in the silica matrix, as a result of further reduction of the nonradiative pathways.

Introduction

The sol−gel process is a promising method for the preparation of bulk materials and thin films used in integrated optics (IO) circuits.[1−3] The major advantages of the process are its simplicity and its ability to control the purity and homogeneity of the final material on a molecular level. The method offers the possibility of modifying the refractive index, phonon energy, and transparency of a material by choosing suitable matrixes such as SiO_2, TiO_2, ZrO_2, Al_2O_3, GeO_2 etc.,[4−8] either individually or in combination. Such matrixes are potential candidates for making planar waveguides, fiber amplifiers, and up-conversion devices, when doped with trivalent lanthanide (also known as rare earth) ions.[9−11] However, improvements are still needed to optimize their performance. The most commonly used lanthanide ion for these applications is Er^{3+}, as it provides amplification in the 1550 nm communication window, through its $^4I_{13/2}\rightarrow{}^4I_{15/2}$ transition. It is desirable to have a high quantum yield and an increased line width for this transition, to enable those materials to be used for broad-band near-infrared amplification. The three main factors which decide the performance characteristics of such lanthanide ion containing materials are the phonon energy of the host in which the lanthanide ions are incorporated, the proximity of the OH groups present in the matrix to the lanthanide ions, and clustering of lanthanide ions. For example in Er^{3+} incorporated materials, high phonon energy of the host matrix favors the nonradiative relaxation of the $^4I_{13/2}$ excited state, thereby reducing its lifetime and quantum yield of the $^4I_{13/2}\rightarrow{}^4I_{15/2}$ transition. Because the OH groups, an inherent result of sol−gel process, quench the excited state of the lanthanide ions by dipole−dipole interaction, the proximity of the OH groups to the lanthanide ions results in a much higher extent of quenching. Finally, clustering of the lanthanide ions reduces the excited-state lifetime by concentration quenching.[12,13] Many reports are available regarding ways to improve the

* To whom correspondence should be addressed. E-mail: fvv@uvic.ca. Phone: +1 250 721 7184. Fax: +1 250 472 5193.

(1) Bhandarkar, S. *J. Am. Ceram. Soc.* **2004**, *87*, 1180.
(2) Moreira, P. J.; Marques, P. V. S.; Leite, A. P. *IEEE Photon. Technol. Lett.* **2005**, *17*, 399.
(3) Davis, R. L.; Long, W., Jr.; Wang, C. J.; Lam, T.; Ho, J. G.; Nachman, P. M.; Poylio, J.; Mishechkin, O. V.; Fallahi, M. *IEEE Photon. Technol. Lett.* **2004**, *16*, 464.
(4) Slooff, L. H.; de Dood, M. J. A.; van Blaaderen, A.; Polman, A. *J. Non-Cryst. Solids* **2001**, *296*, 158.
(5) Chen, S. Y.; Ting, C. C.; Hsieh, W. F. *Thin Solid Films* **2003**, *434*, 171.
(6) Elalamy, Z.; Drouard, E.; Mcgovern, T.; Escoubas, L.; Simon, J. J.; Flory, F. *Opt. Commun.* **2004**, *235*, 365.
(7) Ishizaka, T.; Kurokawa, Y. *J. Appl. Phys.* **2001**, *90*, 243.
(8) Kojima, K.; Tsuchiya, K.; Wada, N. *J. Sol-Gel Sci. Technol.* **2000**, *19*, 511.
(9) Zamperdi, L.; Ferrari, M.; Armellini, C.; Visintainer, F.; Tosello, C.; Ronchin, S.; Rolli, R.; Montagna, M.; Chiasera, A.; Pelli, S.; Righini, G. C.; Monteil, A.; Duverger C.; Goncalves, P. R. *J. Sol-Gel. Sci. Technol.* **2003**, *26*, 1033.
(10) Xiang, Q.; Zhou, Y.; Ooi, B. S.; Lam, Y. L.; Chan, Y. C.; Kam, C. H. *Thin Solid Films* **2000**, *370*, 243.
(11) Bahtat, A.; Marco de Lucas, M. C.; Jacquier, B.; Varvel, B.; Bouazoui, M.; Mugnier, J. *Opt. Mater.* **1997**, *7*, 173.
(12) Lumholt, O.; Rasmissen, T.; Bjarklev, A. *Electron. Lett.* **1993**, *29*, 495.
(13) Blixt, P.; Nilsson, J.; Carlnas, T.; Jaskorzynska, B. *IEEE Photonics Technol. Lett.* **1991**, *3*, 996.

10.1021/cm051065+ CCC: $30.25
Published on Web 08/12/2005

luminescence characteristics of such materials. These mainly include the works of Biswas et al.[14,15] and Tanabe et al.[16] on the sol−gel glasses and glass ceramics containing Er^{3+} ions. These materials have only limited applications as they need to be melted at higher temperature to draw them into fibers. Fiber amplifiers are less convenient for integrated optics because of their increased length, and extensive research is going on to replace them with planar waveguide amplifiers.[17] A lifetime of 17 ms for the $^4I_{13/2}$ level of Er^{3+} was reported by Slooff et al.[18] for Er^{3+} ion implanted silica colloidal particles having sizes in the range of 240−360 nm and annealed over the temperature range of 700−900 °C. This was attributed to the decreased OH concentration in these materials. The disadvantage of this method is that the ion implantation is a small-area, low-throughput procedure.

A general method, from readily available starting materials, that combines the advantage of the improved luminescent properties of Ln^{3+}-doped LaF_3 nanoparticles and the simplicity of making thin films using sol−gel method, is thus highly desirable. In this work a novel method to improve the luminescent properties of lanthanide ions in sol−gel films is reported by isolating the luminescent lanthanide ions from the vibrations of the residual OH groups, reducing the phonon energy of the host, and avoiding clustering of the lanthanide ions. The presented approach is very simple, takes advantage of our work on monolayer-coated Ln^{3+}-doped LaF_3 nanoparticles, and allows for straightforward optimization.[19−23]

A convenient and a straightforward method to incorporate nanoparticles in sol−gel matrix like SiO_2, ZrO_2 etc., requires that the nanoparticles be dispersed in a colloidal state in water. This is achieved by a judicious choice of the stabilizing ligand. Citrate turned out to be a suitable ligand, which on coordination on the surface of the particle makes it soluble in water. The main advantage of the citrate ligand is that it gets completely removed from the matrix as gaseous products without leaving any carbon residues, on heating in air at a relatively low temperature of around 400 °C. The higher-temperature heat treatment is an essential step in the fabrication of sol−gel films as it reduces significantly the OH concentration in the film, thereby reducing the quenching brought about by them. In the present study, LaF_3:Er (5%) nanoparticles stabilized with citrate ligands were prepared and incorporated in silica films made by the sol−gel method. The luminescent aspects of these films were studied as a function of the annealing temperature from 400 to 800 °C. The results were compared with that of silica films doped directly with Er^{3+} ions having the same Er/Si ratio as that of nanoparticle incorporated films. The procedure has been extended to other lanthanide ions such as Nd^{3+} and Ho^{3+} and also to another sol−gel matrix (Al_2O_3), showing the generality of the method.

Experimental Section

Materials. All chemicals were used as received without further purification. The lanthanide salts, $La(NO_3)_3{\cdot}6H_2O$, $Er(NO_3)_3{\cdot}5H_2O$, $Nd(NO_3)_3{\cdot}6H_2O$, $Ho(NO_3)_3{\cdot}5H_2O$ and $Eu(NO_3)_3{\cdot}5H_2O$, all having a purity of 99.99%, tetraethyl orthosilicate, TEOS (99.99%), and sodium fluoride (99%) were purchased from Aldrich. Citric acid (99%) was purchased from Caledon Laboratories Ltd.

Preparation of Core Nanoparticles. LaF_3:Er, LaF_3:Nd, LaF_3:Ho, and LaF_3:Eu nanoparticles (all doped at 5 atom % with respect to the total amount of lanthanide ions), stabilized with citrate ligand, were prepared by the coprecipitation technique in aqueous solution in the presence of citrate ions. Around 2 g of citric acid and 0.126 g of NaF was dissolved in 40 mL of water. The pH of the solution was adjusted to 6 by adding NH_4OH, and the solution was heated to 75 °C. Stoichiometric amounts of the nitrate salts of lanthanide ions were dissolved in 2 mL of water (for Er^{3+} and Eu^{3+} ions) or 2 mL of methanol (for Nd^{3+} and Ho^{3+} ions) and added dropwise. A clear solution was obtained, and after 2 h of reaction, the resulting solution was mixed with 75 mL of ethanol to precipitate the nanoparticles. These particles were collected by centrifugation, washed with ethanol, and dried under vacuum.

Preparation of Core−Shell Nanoparticles. Around 3 g of citric acid was dissolved in 35 mL of water and neutralized with NH_4OH till the pH reached around 6, and this solution was then heated to 75 °C. $La(NO_3)_3{\cdot}6H_2O$ and $Nd(NO_3)_3{\cdot}6H_2O$ or $Ho(NO_3)_3{\cdot}5H_2O$ (1.33 mmol total) were dissolved in 3 mL of methanol and added to this followed by the dropwise addition of 3 mL of water containing 0.266 g of NaF. After 10 min, 3 mL of a methanolic solution containing 0.6 g of $La(NO_3)_3{\cdot}6H_2O$ was added dropwise to the reaction mixture while stirring, for the formation of shell around the core particles. The reaction was allowed to continue for 2 h and finally the nanoparticles were precipitated by the addition of excess of ethanol to the reaction mixture. They were collected by centrifuge and dried for 24 h.

NMR Measurements. The room-temperature ^1H NMR pattern was recorded using a Bruker AC 300 instrument. The basic frequency for the ^1H nucleus is 300.13 MHz. ^1H NMR of LaF_3:Eu particles stabilized with citrate ligand δ (D_2O): 2.45−2.60 (broad, $CH_2COOH - COH(COOH) - CH_2COOH$).

AFM Measurements. AFM images were recorded in the contact mode using a Thermo microscope AFM scanner having a silicon nitride tip (model MLCT-EXMT-A) supplied by Veeco Instruments. The particles were dissolved in water and a drop of the solution was put on a mica sheet (5×5 mm^2) and allowed to dry before the sheet was mounted on the sample holder. The measurements were done with a resolution of 500×500 pixels per image and an image dimension of 5×5 μm^2. The average particle height was determined by measuring the individual particle heights for over 100 particles.

Incorporation of Nanoparticles in Silica Films. Around 50−60 mg of these nanoparticles was dissolved in 1.5 mL of water, which was then mixed with 3 mL of tetraethyl orthosilicate (TEOS) and 7.8 mL of ethanol. The pH of the solution was adjusted to 2 by adding few drops of 0.1 N HCl and the solution was stirred for 24 h to get a clear sol. The sol was then spin coated on a quartz

(14) Biswas, A.; Maciel, G. S.; Kapoor, R.; Friend, C. S.; Prasad, P. N. *Appl. Phys. Lett.* **2003**, *15*, 2389.
(15) Biswas, A.; Maciel, G. S.; Kapoor, R.; Friend, C. S.; Prasad, P. N. *J. Non-Cryst. Solids* **2003**, *316*, 393.
(16) Tanabe, S.; Hayashi, H.; Hanada, T.; Onodera, N. *Opt. Mater.* **2002**, *19*, 343.
(17) Yeatman, E. M.; Ahmad, M. M.; Mccarthy, O.; Martucci A.; Guglielmi, M. *J. Sol-Gel. Sci. Technol.* **2000**, *19*, 231.
(18) Slooff, L. H.; de Dood, M. J. A.; van Blaaderen, A.; Polman, A. *Appl. Phys. Lett.* **2000**, *76*, 3682.
(19) Stouwdam, J. W.; van Veggel, F. C. J. M. *Nano Lett.* **2002**, *2*, 733.
(20) Hebbink, G. A.; Stouwdam, J. W.; Reinhoudt, D. N.; van Veggel, F. C. J. M. *Adv. Mater.* **2002**, *14*, 1147.
(21) Stouwdam, J. W.; Hebbink, G. A.; Huskens, J.; van Veggel, F. C. J. M. *Chem. Mater.* **2003**, *15*, 4604.
(22) Sudarsan, V.; van Veggel, F. C. J. M.; Herring, R. A.; Raudsepp, M. *J. Mater. Chem.* **2005**, *15*, 1332.
(23) Stouwdam, J. W.; van Veggel, F. C. J. M. *Langmuir* **2004**, *20*, 11763.
(24) Weber M. J. *Phys. Rev.* **1967**, *156*, 231.
(25) Weber M. J. *Phys. Rev.* **1967**, *157*, 262.

substrate at 2500 rpm and heated at different temperatures under ambient environment.

Incorporation of Nanoparticles in Al_2O_3 Films. Al_2O_3 sols were prepared based on the procedure similar to that of Ishizaka et al.[26] Hydrous aluminum hydroxide was precipitated by adding aqueous 6 M NH_3 solution to a 0.2 M $Al(NO_3)_3 \cdot 9H_2O$ solution dropwise under stirring. The precipitated hydroxide was aged for 12 h without stirring, then centrifuged and washed with water. This was then mixed with glacial acetic acid and heated at 80 °C for 8 h to get a viscous sol. Around 2 mL of the viscous sol was mixed with around 3.5 mg of $Er(NO_3)_3 \cdot 5H_2O$ or around 30 mg of LaF_3:Er nanoparticles stabilized with citrate ligand and stirred for 24 h. The sol was then spin coated on a quartz substrate at 2500 rpm and heated at 800 °C in air for 8 h.

Luminescence Studies. Photoluminescence measurements in the near-infrared region (NIR) were recorded with an Edinburgh Instruments' FLS 920 instrument attached with a Vibrant tunable laser system (model 355 II) having a Quantel Nd:YAG nanosecond pump laser as the excitation source and a nitrogen-gas-cooled Hamamatsu R5509 NIR PMT as the detector. The emission spectra were corrected for the detector response. For recording the spectra in the visible region, a 450-W Xe arc lamp and a red-sensitive Peltier element cooled Hamamatsu R928-P PMT were used as the excitation source and detector, respectively. The decay curves were recorded with 5-ns laser pulses with a repetition frequency of 10 Hz.

Powder X-ray Diffraction Studies. Approximately 20−25 mg of the sample was powdered in an alumina mortar to break up lumps. The powder was smeared onto a zero-diffraction quartz plate using ethanol. Step-scan X-ray powder-diffraction data were collected over the 2θ range 3−100° with Cu Kα (40 kV, 40 mA) radiation on a Siemens D5000 Bragg−Brentano $\theta-2\theta$ diffractometer equipped with a diffracted-beam graphite monochromator crystal, 2-mm (1°) divergence and anti-scatter slits, 0.6-mm receiving slit, and incident beam Soller slit. The scanning step size was 0.04° 2θ with a counting time of 2 s/step. X-ray powder-diffraction data for different phases were refined with the Rietveld program Topas 2.1 from Bruker using the fundamental parameters approach.[27]

Results and Discussion

Formation of citrate-stabilized LaF_3:Ln nanoparticles has been confirmed from ^{1}H NMR and AFM images of the nanoparticles after they were dispersed in water. The broad NMR peak observed around 2.6 ppm (Figure 1 of the Supporting Information) is characteristic of the protons of the citrate ligand coordinated on the surface of the nanoparticle. The broadening is ascribed to the inhomogeneous distribution of the magnetic environment around nanoparticles and a reduction in the rotational freedom of the ligand.[28,29] The majority of the particles have heights in the range of 3−7 nm as can be seen from the AFM image of a representative LaF_3:Er sample (Figure 2 of the Supporting Information).

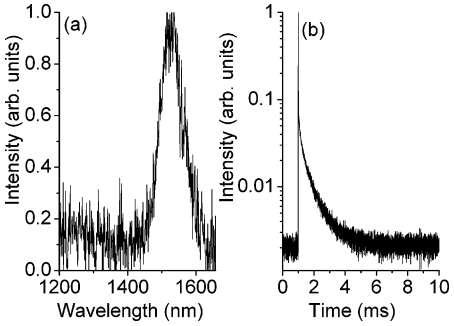

Figure 1. Emission spectrum (a) and decay curve (b) for LaF_3:Er-citrate particles dissolved in D_2O. The sample was excited at 488 nm and the emission was monitored at 1530 nm.

An emission spectrum of a D_2O solution of citrate-stabilized LaF_3:Er nanoparticles is shown in Figure 1a. The broad peak around 1530 nm with a full width at half-maximum (fwhm) = 69 nm corresponds to the $^4I_{13/2} \rightarrow {}^4I_{15/2}$ transition characteristic of Er^{3+}. The decay curve corresponding to the $^4I_{13/2}$ level of Er^{3+} in the sample is shown in Figure 1b and this could be fitted biexponentially with decay times 200 μs (82%) and 58 μs (18%), respectively. In some previous papers we have discussed the origin of the multi-exponential decay curves.[19−23] The decay times are characteristic of Er^{3+} when incorporated in nanoparticles of low phonon energy hosts such as LaF_3.[21] They are certainly much lower than in single crystals of LaF_3 doped with Er^{3+}, albeit at lower concentrations.[24,25] The reason for our relatively short lifetimes is due to significant quenching by molecules on the surface, citrate, and D_2O. Concentration quenching is probably not a major contribution as our results in the sol−gel thin films show (see below).

The citrate stabilized LaF_3:Er nanoparticles were then incorporated in sol−gel films and subjected to annealing at different temperatures. The films were transparent to visible light and no cracks were observed. The thickness evolution of the films with annealing temperatures and variation of refractive index of the films with particle concentrations have been discussed in a recent communication.[30]

Figure 2 shows the emission spectra and decay curves for the LaF_3:Er and Er^{3+} incorporated silica films with Er/Si ratio 1.0×10^{-3} and heated in air at 400, 600, and 800 °C, respectively, for 12 h. There is a significantly improved signal-to-noise ratio in the emission spectrum for the particle-incorporated films heated at all the temperatures. Furthermore, the full width at half-maximum (fwhm) values for particle-incorporated films are almost comparable for all the heat treatment temperatures. However, for silica films directly incorporated with Er^{3+} ions the signal-to-noise ratio was poor, particularly for low-temperature heat-treated films, and the line width drastically reduces with increase in heat treatment temperatures. The lifetime values corresponding to the $^4I_{13/2}$ level of Er^{3+} from the 800 °C heated samples are shown in Table 1. Corresponding values for the low-temperature heated films are shown in Table 2. For silica films incorporated with LaF_3:Er nanoparticles, lifetime values are much higher at all the heat treatment temperatures compared to

(26) Ishizaka, T.; Kurokawa, Y. *J. Lumin.* **2001**, *92*, 57.
(27) Bruker AXS. *Topas V2.1: General Profile and Structure Analysis Software for Powder Diffraction Data − User's Manual*; Bruker AXS,: Karlsruhe, Germany, 2003.
(28) Kuno, M.; Lee, J. K.; Dabbousi, B. O.; Mikulec, F. V.; Bawendi, M. G. *J. Chem. Phys.* **1997**, *106*, 9869.
(29) Sachleben, J. R.; Wooten, E. W.; Emsley, L.; Pines, A.; Colvin, V. L.; Alivisatos, A. P. *Chem. Phys. Lett.* **1992**, *198*, 431.
(30) Dekker, R.; Sudarsan, V.; van Veggel, F. C. J. M.; Worhoff, K.; Driessen, A. *Proc. Symp. IEEE/LEOS Benelux Chapter* **2004**, 295.

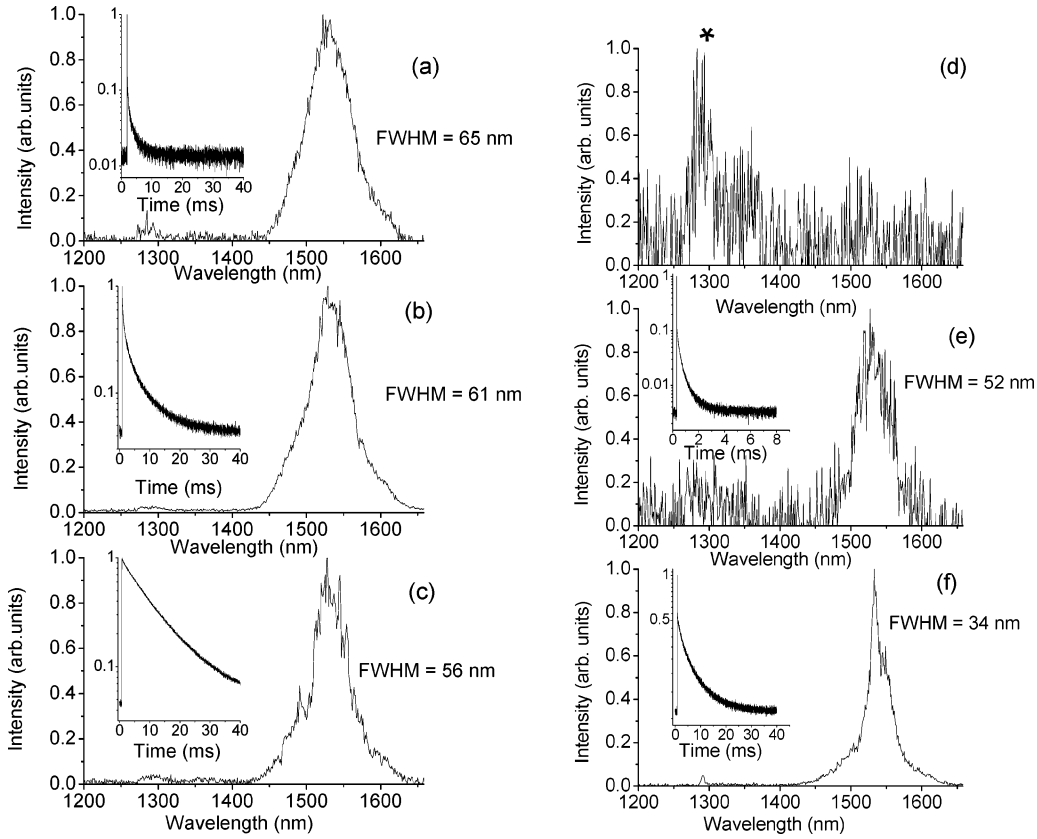

Figure 2. Emission spectra and decay curves for silica films containing LaF_3:Er nanoparticles (left) and bare Er^{3+} ion (right) with Er/Si = 1×10^{-3} and heated in air for 12 h at (a and d) 400, (b and e) 600, and (c and f) 800 °C. The samples were excited at 488 nm and emission was monitored at 1532 nm. Peak marked "*" is an artifact.

Table 1. Lifetimes in ms for Er^{3+} ($^4I_{13/2}$), Nd^{3+} ($^4F_{3/2}$) and Ho^{3+} ($^5F_3$) Ions in Silica Films When Incorporated as Nanoparticles and Bare Ions (All the Samples Were Heated at 800 °C and the Numbers in Brackets Indicate the Relative Percentages of the Different Lifetime Components)

	LaF_3:Ln−SiO_2 Films[a]					
	Core		Core−Shell		Ln−SiO_2 Films[a]	
Ln^{3+}	τ_1	τ_2	τ_1	τ_2	τ_1	τ_2
Er^{3+}	10.9 (95)	3.9 (5)	*b*	*b*	6.0 (70)	1.2 (30)
Nd^{3+}	0.171 (72)	0.056 (28)	0.325 (76)	0.087 (24)	0.130 (52)	0.002 (48)
Ho^{3+}	0.006 (75)	0.012 (25)	0.007 (65)	0.015 (35)	*c*	*c*

[a] Er/Si = 1.0×10^{-3}, Nd/Si = 0.9×10^{-3}, and Ho/Si = 1.5×10^{-3}. [b] Measurements could not be done as the films were of poor quality. [c] No emission observed.

Table 2. Lifetime Values of Er^{3+} ($^4I_{13/2}$) Ions in Silica Films When Incorporated as Nanoparticles and Bare Ions and Heated at Different Temperatures (Numbers in Brackets Give the Relative Percentages of the Two Lifetime Components)

	LaF_3:Er−SiO_2 films Er/Si = 1×10^{-3}		Er^{3+}−SiO_2 films Er/Si = 1×10^{-3}	
temperature (°C)	τ_1 ms (%)	τ_2 ms (%)	τ_1 ms (%)	τ_2 ms (%)
400	2.6 (70%)	0.6 (30%)	*a*	*a*
600	7.4 (69%)	0.9 (31%)	0.98 (35%)	0.27(65%)

[a] No emission observed.

the directly Er^{3+} incorporated silica films, as can be seen from Figure 2 and Tables 1 and 2. For nanoparticle-incorporated films heated at 800 °C, the $^4I_{13/2}$ lifetime was found to be 10.9 ms, which to our knowledge is the highest value reported for silica films containing Er^{3+} ions, *heated in air*. In the case of silica film incorporated with bare Er^{3+} ions and heated at 800 °C, there is a fast decay component followed by a slow decay component. Lanthanide ions such as Er^{3+}, Nd^{3+}, etc., have been demonstrated to undergo clustering when incorporated in the silica matrix, and addition of an oxide such as Al_2O_3 reduces the clustering effect.[31−33] Clustered rare earth ions have a shorter lifetime compared to the nonclustered ones.[34] Thus the observed fast decay component for the 800 °C heated film has been attributed to the aggregation of Er^{3+} ions in the silica matrix. However, for silica films incorporated with LaF_3:Er nanoparticles, no fast decay component was observed particularly for the ones heated at 600 and 800 °C. Thus, the particle-incorporated silica films offer a clear advantage in terms of the improved lifetime and absence of clustering of lanthanide ions when compared with silica films directly incorporated with the bare Er^{3+} ion.

Similar experiments were carried out for Nd^{3+}- and Ho^{3+}-incorporated samples. The citrate-stabilized nanoparticles of

(31) Costa, V. C.; Lochhead, M. J.; Bray, K. L. *Chem. Mater.* **1996**, *8*, 783.
(32) Laegsgaard, J. *Phys. Rev. B* **2002**, *65*, 174114.
(33) Legendziewicz, J.; Streak, W.; Sokolnicki, J.; Hreniak, D.; Zolin, V. *Opt. Mater.* **2002**, *19*, 175.
(34) Langlet, M.; Coutier, C.; Meffre, W.; Audier, M.; Fick, J.; Rimet, R.; Jacquier, B. *J. Lumin.* **2002**, *96*, 295.

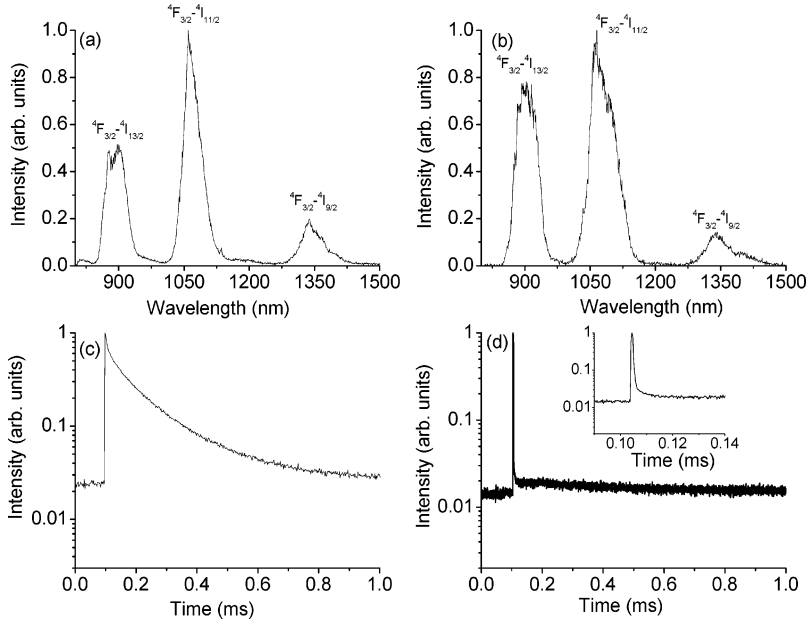

Figure 3. Emission spectra and decay curves for 800 °C heated (12 h) silica films containing LaF_3:Nd nanoparticles (a and c) and bare Nd^{3+} ions (b and d), with Nd/Si ratio = 0.9×10^{-3}. The samples were excited at 514 nm and emission was monitored at 1064 nm. The inset of the decay curve in (d) shows an expansion of the fast decay component.

LaF_3:Nd and LaF_3:Ho were incorporated in a silica matrix by the same procedure employed for the LaF_3:Er nanoparticles. Figure 3 shows the emission spectra and corresponding decay curves for silica films incorporated with LaF_3:Nd nanoparticles and Nd^{3+} ions, respectively, with a Nd/Si ratio 0.9×10^{-3}, and heated at 800 °C in air for 12 h. For silica films doped with LaF_3:Nd nanoparticles, decay corresponding to $^4F_{3/2}$ level is multiexponential with a major component of ~171 μs (72%). For Nd^{3+} ions directly doped in silica films with the same Nd/Si ratio, the corresponding decay curve is characterized by a fast decay component (~2.0 μs, 48%) as can be seen from the inset of Figure 3d, and a slow decay component (130 μs, 52%). The fast component is attributed to the clusters of Nd^{3+} ions formed in the silica matrix.[34] A comparison of the lifetime values shown in Table 1 and the decay curves shown in Figure 3 clearly reveals that there is an improvement of the luminescent properties, in terms of improved lifetime and absence of lanthanide ion clustering, when the nanoparticles are incorporated in the silica films rather than the bare ions.

For silica films incorporated with LaF_3:Ho nanoparticles with a Ho/Si ratio around 1.5×10^{-3} and heated at 800 °C, luminescence was observed both in the visible and near-infrared regions. The emission spectrum in the near-infrared region along with the decay curve corresponding to the $^5F_3$ level of Ho^{3+} from this sample is shown in Figure 4. The lifetime value of $^5F_3$ level was found to be 6 μs (75%) and 12 μs (25%), with no faster decay component, indicating the absence of Ho^{3+} clustering in the sample. In contrast to this, when Ho^{3+} ions were directly doped in silica films with the same Ho/Si ratio, no emission was observed in the visible and near-infrared regions. (The emission in the visible region and the corresponding decay curve for the nanoparticle-incorporated silica films heated at 800 °C are shown in Figure 3 of the Supporting Information.)

With a view to understanding the chemical changes taking place with the lanthanide ions and the nanoparticle matrix,

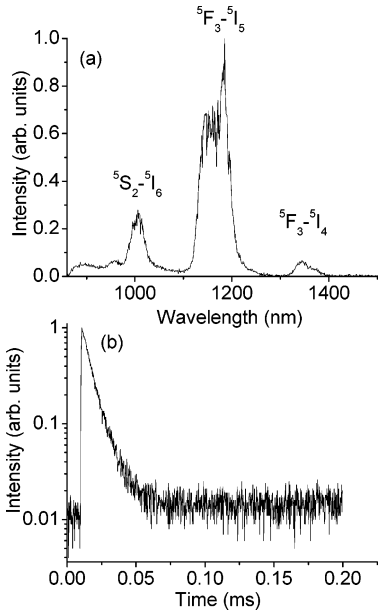

Figure 4. Emission spectrum (a) and decay curve (b) for silica films containing LaF_3:Ho nanoparticles with Ho/Si ratio = 1.5×10^{-3} and heated in air at 800 °C for 12 h. The samples were excited at 448 nm with emission monitored at 1180 nm ($^5F_3$ to $^5I_5$ transition).

LaF_3:Eu nanoparticle stabilized with citrate ligands have been prepared, incorporated in silica matrix, and subjected to heat treatments at different temperatures. Figure 5a shows the emission spectra of the LaF_3:Eu nanoparticle incorporated silica film heated at 800 °C in air. The intensity of the $^5D_0 \rightarrow {}^7F_2$ emission peak (~615 nm) for this sample was found to be significantly larger than that of the $^5D_0 \rightarrow {}^7F_1$ emission peak (591 nm), which is characteristic of Eu^{3+} surrounded by oxygen ions.[35] As both $^5D_0$ and $^7F_0$ levels are nondegenerate, the transition between the levels can be used as a probe

(35) Cannas, C.; Casu, M.; Mainas, M.; Musinu, A.; Piccaluga, G.; Polizzi, S.; Speghini A.; Bettinelli, M. *J. Mater. Chem.* **2003**, *13*, 3079.

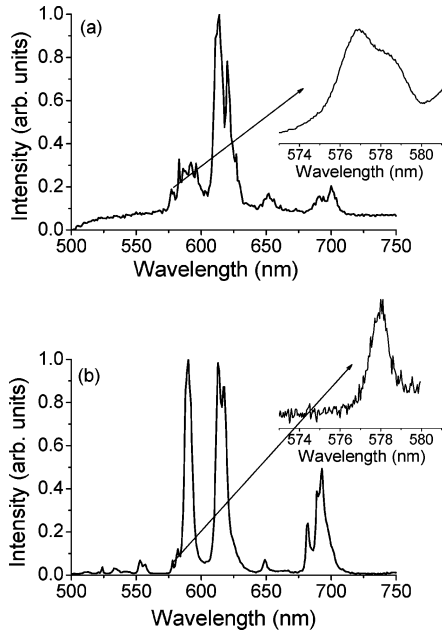

Figure 5. Emission spectra of (a) LaF_3:Eu nanoparticle incorporated silica film heated at 800 °C in air for 12 h, and (b) LaF_3:Eu-citrate nanoparticles dissolved in water. (The insets show the emission spectrum collected with a resolution of 0.2 nm in the region corresponding to $^5D_0 \rightarrow {}^7F_0$ transition). The samples were excited at 464 nm.

to understand the environment around the Eu^{3+} ions in the lattice. The high-resolution emission spectrum corresponding to the $^5D_0 \rightarrow {}^7F_0$ transition for LaF_3:Eu nanoparticles incorporated silica films (shown as inset of Figure 5a) clearly shows an asymmetric peak which could be deconvoluted into two Gaussians centered around 576.9 and 578.2 nm, respectively, indicating that more than one type of Eu^{3+} is present in the films. For LaF_3:Eu nanoparticles a relatively sharper and more symmetric peak around 578 nm was observed corresponding to the $^5D_0 \rightarrow {}^7F_0$ transition (inset of Figure 5b). Comparing the spectra in Figure 5a and b, it is clear that Eu^{3+} exists in more than one crystallographic phase in LaF_3:Eu incorporated silica films. X-ray diffraction studies carried out on a sample of silica film incorporated with 25 wt % of LaF_3:Eu nanoparticles and heated at 800 °C in air for 12 h revealed the presence of a nonstoichiometric lanthanum silicate phase ($La_{9.31}Si_{6.24}O_{26}$)[36] along with the expected LaF_3 phase as can be seen from Figure 6, roughly in a 1:1 ratio. The Eu^{3+} thus occurs in two different phases, which confirms the luminescence data. It is likely that the surface of the LaF_3:Eu nanoparticles has reacted with the silanol groups of the matrix to form the Eu^{3+}-doped lanthanum silicate surrounding a core of unreacted LaF_3:Eu. We assume that the same occurs for all LaF_3:Ln (Ln: Er, Nd, and Ho) doped SiO_2 films in this study.

The lifetime values of the lanthanide ion containing silica films can be further improved by incorporating the core−shell nanoparticles that have a doped core covered by an undoped shell. Formation of nanoparticles having a core−shell geometry by the procedure mentioned in the Experimental Section has been confirmed from the luminescent studies of citrate-stabilized LaF_3:Eu−LaF_3 core−shell nanoparticles, prepared by the same procedure. Unlike the core LaF_3:Eu nanoparticles, for the core shell LaF_3:Eu−LaF_3

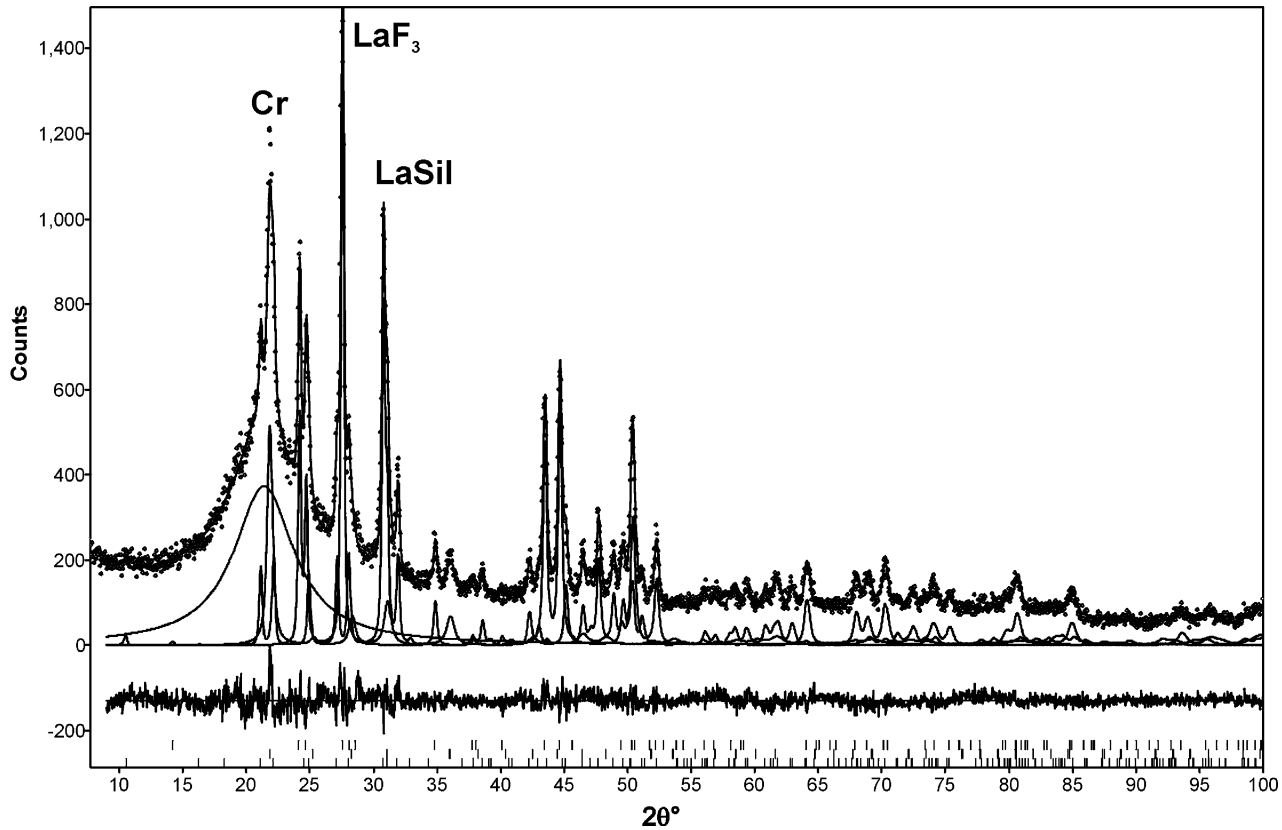

Figure 6. XRD pattern (Rietveld refinement plot) of a 25 wt % of LaF_3:Eu (5%) nanoparticles incorporated silica film heated at 800 °C for 12 h in air. Diamonds: observed pattern; solid line: calculated pattern; solid lines below: calculated patterns of individual phases (selected peaks shown for Cr, cristobalite, LaF_3, LaF_3 phase, LaSil, $La_{9.31}Si_{6.24}O_{26}$ phase); and solid line bottom: difference pattern. The broad peak around 22 degrees is attributed to amorphous silica.

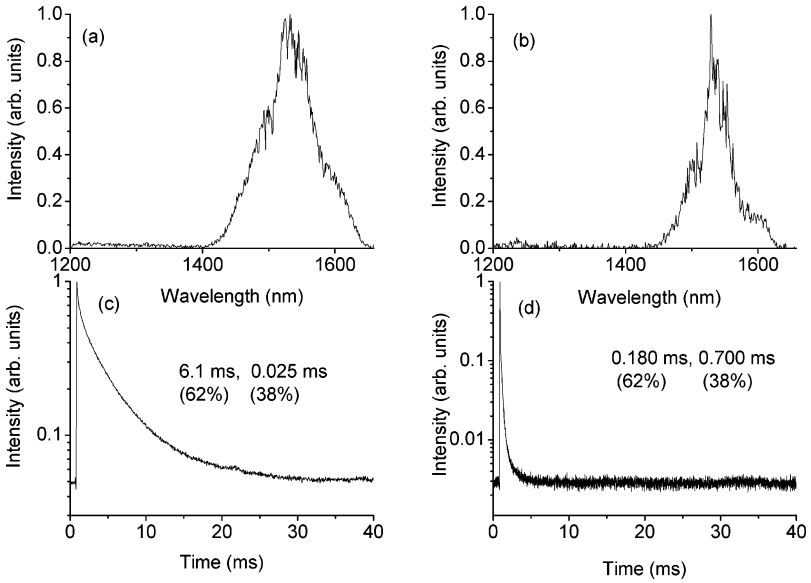

Figure 7. Emission spectra and decay curves for 800 °C heated (12 h) alumina films containing LaF_3:Er nanoparticles (a and c) and bare Er^{3+} ions (b and d), with the ratio Er/Al = 1.5×10^{-3}. The samples were excited at 488 nm and emission was monitored at 1532 nm.

nanoparticles, as the surface Eu^{3+} ions are well covered by the undoped LaF_3 shell, Eu^{3+} ions will have a more symmetric crystal field around them and hence the decay curve corresponding to the $^5D_0$ level of Eu^{3+} is single exponential.[22,23] Further due to the same reason, the relative intensity ratio of the 612−590 nm peak (also known as the asymmetric ratio) in the emission spectrum of core−shell nanoparticles is lower compared to the core nanoparticles. This can be indeed seen from the emission spectra and the decay curves for both the LaF_3:Eu core and LaF_3:Eu−LaF_3 core shell nanoparticles stabilized with citrate ligands, shown in Figure 4 of the Supporting Information. Core−shell nanoparticles doped with Er^{3+} ions in the core were found to be less soluble in water and hence good quality sol−gel films could not be obtained. This aspect is currently under investigation. The lifetime values observed for $^4F_{3/2}$ level of Nd^{3+} and $^5F_3$ level of Ho^{3+} in LaF_3:Nd−LaF_3 and LaF_3:Ho−LaF_3 core−shell nanoparticle incorporated films are shown in Table 1. There is an improvement in the lifetime for the core−shell nanoparticle incorporated films compared to the core nanoparticle incorporated films.

To further substantiate the generality of the method, the above experiments were repeated by taking Al_2O_3 as the sol−gel matrix. Similar to SiO_2 matrix, significant improvements in the lifetime values were observed when LaF_3:Er nanoparticles were incorporated in the films compared to the bare Er^{3+} incorporated films as can be seen from Figure 7.

Conclusions

In conclusion, a general method, from readily available and cheap starting materials, that combines the advantages of both nanoparticles and the sol−gel method, has been demonstrated for making silica and alumina films containing highly luminescent lanthanide ions. The improved luminescent properties of nanoparticle incorporated films have been attributed to the effective isolation of lanthanide ions from the high phonon energy matrix, residual OH groups, and absence of lanthanide ion clustering. We are currently extending this easy method to other luminescent Ln^{3+} ions, other nanoparticles, and other matrixes (e.g., TiO_2 and ZrO_2).

Acknowledgment. We are grateful for the financial support received from NSERC to conduct this work and to CFI/BCKDF for the financial support of the infrastructure.

Supporting Information Available: ^{1}H NMR spectrum and AFM image of the citrate stabilized LaF_3:Er nanoparticles, visible emission spectrum and decay curve of LaF_3:Ho in SiO_2 thin films, and emission spectrum and decay curves of core and core shell LaF_3:Eu nanoparticles dispersed in water. This material is available free of charge via the Internet at http://pubs.acs.org.

(36) Kalsbeek, N.; Larsen, S. *Z. Kristallogr.* **1990**, *191*, 249.

CM051065+